

Density Functional Theory: from theory to Applications

Marialore Sulpizi

Uni Mainz

May 14, 2012

Solving the electronic problem in practice

All electrons vs pseudopotentials

Classes of Basis-set

Condensed phase: Bloch's th and PBC

Pseudopotentials

Hamann-Schlüter-Chiang pseudopotentials

Bachelet, Kerker, Martin-Troulliers

Thermostats

Thermostat on the electrons

Nose'-Hoover chain thermostat

Imposing pressure: barostats

Alternative approach for clusters

Solving the electronic problem in practice

All electrons vs pseudopotentials

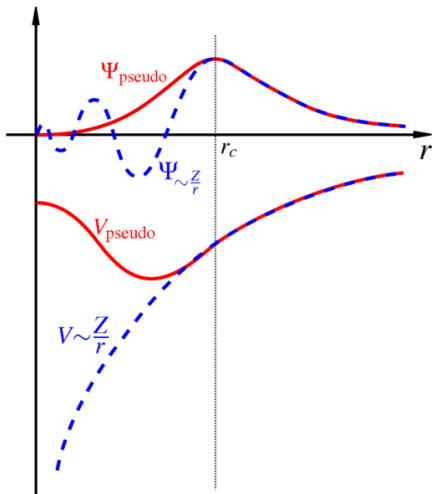
There are two classes of electrons: *valence electrons* (participate to chemical bonds) and *core electrons* (tightly bound to the nuclei). Eventually *semi-core electrons* (close in energy to valence states to feel the presence of the environment)

All-electron methods

- ▶ fixed orbital basis set: core electron minimal number of basis function to reproduce atomic features, valence and semi-core more complete basis set to describe the chemical bond.
- ▶ augmented basis set. Divide the space into spherical regions around the atoms and interstitial regions and requesting that the basis functions are continuous and differentiable across the boundaries.

Pseudopotential methods

- ▶ Core electrons are eliminated. Nuclei effective charge $Z_V = Z - Z_{core}$.
- ▶ Number of electron treated explicitly is reduced
- ▶ The bare Coulomb potential is replaced by a screened Coulomb potential
- ▶ Inner solution, inside the core radius, is replaced with a smooth, node-less pseudo-wave function
- ▶ Pseudopotentials are usually chosen to be dependent on the angular momentum.
E.g. for Pt 6p orbitals are quite external and peaked at around 3.9Å, the 6s peak at around 2.4 Å and the main peak of 5d is located at 1.3 Å.



Classes of Basis-set

- ▶ *Extended basis set*: delocalized, such as plane waves, useful for condensed phase systems. Tends to be inefficient for molecular systems.
- ▶ *Localized basis set*: mainly centered at the atomic positions (but also at position of "ghost" atoms). Mainly used for molecular systems
- ▶ *Mixed basis set*: designed to take best of the two worlds (delocalized + localized). There can be some technical issues (over-completeness).
- ▶ *Augmented basis set*: where an extended or atom centered basis set is augmented with atomic like wf in spherical regions around the nuclei.

Condensed phase: Bloch's th and PBC

Condensed phase: problem of choosing the size of the simulation cell. For periodic system: unit of Wigner-Seitz cell, the minimal choice that contains the whole symmetry of the system. Sometimes it is convenient to choose a larger cell to simplify description of symmetry properties. In an external periodic potential $v(\mathbf{r}) = v(\mathbf{r} + \mathbf{a}_i)$ the wf can be written as:

$$\psi_k(\mathbf{r}) = e^{i\mathbf{k}\cdot\mathbf{r}} u_k(\mathbf{r}) \quad (1)$$

with $u_k(\mathbf{r}) = u_k(\mathbf{r} + \mathbf{a}_i)$.

$$\psi_k(\mathbf{r} + \mathbf{a}_i) = e^{i\mathbf{k}\cdot\mathbf{a}_i} \psi_k(\mathbf{r}) \quad (2)$$

So that the probability density is $|\psi_k(\mathbf{r})|^2$ is exactly the same.

Looking at

$$\psi_{\mathbf{k}}(\mathbf{r} + \mathbf{a}_i) = e^{i\mathbf{k} \cdot \mathbf{a}_i} \psi_{\mathbf{k}}(\mathbf{r})$$

we notice that there is a class of vectors \mathbf{k} such that

$$e^{i\mathbf{k} \cdot \mathbf{a}_i} = 1 \quad (3)$$

The reciprocal lattice vectors are defined by

$$\mathbf{a}_i \cdot \mathbf{b}_j = 2\pi \delta_{ij} \quad (4)$$

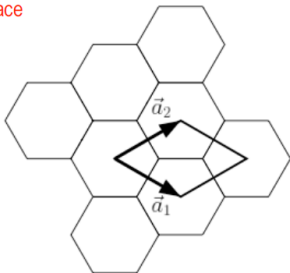
and

$$\mathbf{b}_1 = 2\pi \frac{\mathbf{a}_2 \times \mathbf{a}_3}{\Omega}; \quad \mathbf{b}_2 = 2\pi \frac{\mathbf{a}_3 \times \mathbf{a}_1}{\Omega}; \quad \mathbf{b}_3 = 2\pi \frac{\mathbf{a}_1 \times \mathbf{a}_2}{\Omega} \quad (5)$$

The reciprocal lattice vectors define the first Brillouin Zone (BZ).

- Example: honeycomb lattice

real space

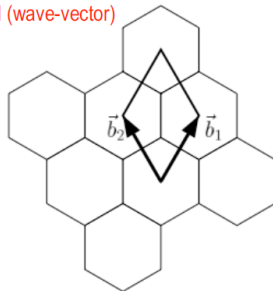


Lattice vectors a_1, a_2, a_3

Unit cell volume Ω

Crystallographic basis consisting of two atoms

Reciprocal (wave-vector) space



Reciprocal-lattice vectors b_1, b_2, b_3 , each perpendicular to a pair of lattice vectors

$$\vec{b}_i = \frac{2\pi}{\Omega} (\vec{a}_j \times \vec{a}_k)$$

Bloch's theorem indicates that it is not necessary to determine the electronic wavefunction everywhere in space. It is sufficient to know the solution in the unit cell.

Using the fact that a periodic function can be represented by a Fourier series:

$$\psi_{\mathbf{k}}(\mathbf{r}) = e^{i\mathbf{k}\cdot\mathbf{r}} \sum_{\mathbf{G}} C_{\mathbf{k}+\mathbf{G}} e^{i\mathbf{G}\cdot\mathbf{r}} \quad (6)$$

where the sum is over $G = n_1\mathbf{b}_1 + n_2\mathbf{b}_2 + n_3\mathbf{b}_3$, the reciprocal lattice vectors.

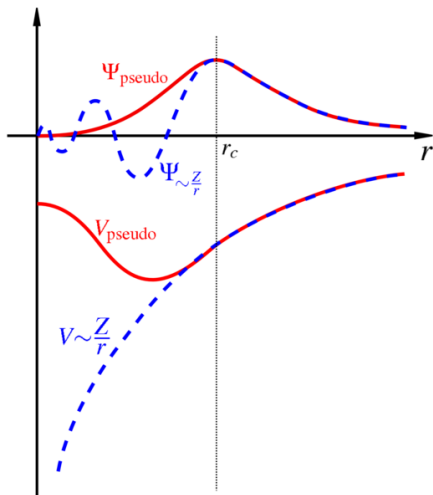
\mathbf{k} is restricted to all the vectors in the first Brillouin zone. In practice calculations are done only for a finite number of \mathbf{k} .

The number of \mathbf{k} points depends on the systems we want to study.

Aperiodic systems: molecules, surfaces and defects

- ▶ supercell approach with PBC, making sure that required physical and chemical properties are converged with respect to the size of the supercell.
- ▶ For surfaces and molecules, e.g., introduce a vacuum region large enough that there is no interaction between images.
- ▶ For charged systems difficulties due to the electrostatic interactions (long range). A uniform neutralizing background is introduced.

- ▶ Only the chemically active electrons are considered explicitly.
- ▶ The core electrons are eliminated within the frozen-core approximation and are considered together with the nuclei as rigid non-polarizable ion cores.
- ▶ The Pauli repulsion largely cancels the attractive parts of the true potential in the core region, and is built into the therefore rather weak pseudopotentials.

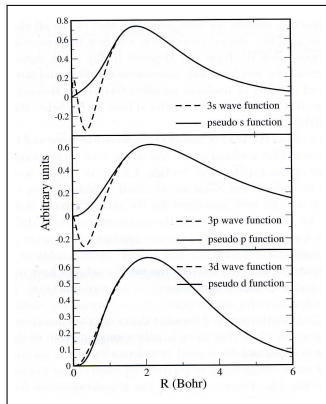


Why Pseudopotentials?

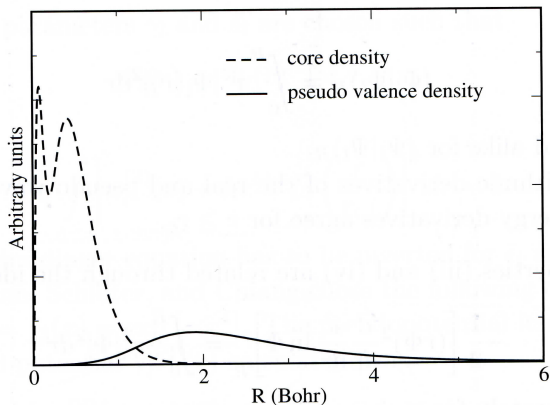
- ▶ Reduction of the number of electron in the systems, faster calculation for large systems
- ▶ Relativistic effects depending on the core electrons treated incorporated indirectly in the pseudopotentials
- ▶ In the frame of plane wave basis set: reduction of the basis set size introducing smoother functions which requires a lower cutoff
- ▶ The number of plane waves needed for a certain accuracy increases with the square of the nuclear charge.

Norm-conserving pseudopotentials

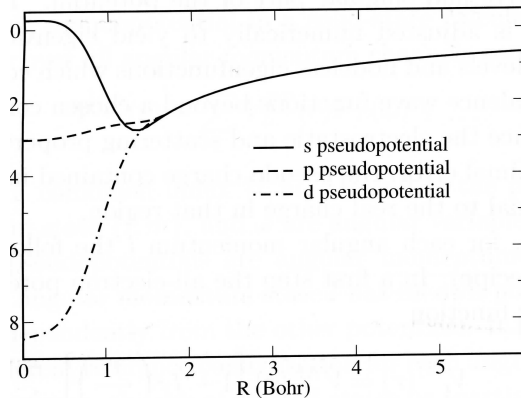
Norm-conserving pseudopotentials conserves the normalization of the pseudo wf in the core region so that the wf outside resembles that of the all-electrons as closely as possible.



Valence and pseudo wf of a Si atom, generated according to Martin-Troullier scheme.



Ground state core density (dashed line) and pseudo valence density (solid line) for a Si atom.



Note: The pseudopotentials converge to the limit $-Z/r$ outside the core radius.

Hamann-Schlüter-Chiang conditions¹

Norm-conserving pseudos are derived from atomic reference state:


$$(T + V^{AE})|\Psi_I\rangle = \epsilon_I|\Psi_I\rangle. \quad (7)$$

This is replaced by the "valence electrons only"

$$(T + V^{val})|\Phi_I\rangle = \tilde{\epsilon}_I|\Phi_I\rangle. \quad (8)$$

Imposing the following:

- ▶ $\epsilon_I = \tilde{\epsilon}_I$ for a chosen prototype atomic configuration.
- ▶ $\Psi_I(r) = \Phi_I(r)$ for $r \geq r_c$.
- ▶ Norm conservation, $\langle \Phi_I | \Phi_I \rangle_R = \langle \Psi_I | \Psi_I \rangle_R$ for $R \geq r_c$.
- ▶ Log derivative of Φ_I equal to that of Ψ_I .

¹Hamann-Schlüter-Chiang, *Phys. Rev. Lett.*, 43, 1494 (1979) 

Hamann-Schlüter-Chiang recipe

- ▶ First step: the all-electron wf is multiplied by a smoothing function f_1 to remove strongly attractive and singular part of the potential:

$$V_l^{(1)}(r) = V^{AE}(r) \left[1 - f_1 \left(\frac{r}{r_{c,l}} \right) \right] \quad (9)$$

- ▶ Then a function f_2 is added in order to obtain $\epsilon_l = \tilde{\epsilon}_l$

$$V_l^{(2)}(r) = V_l^{(1)}(r) + c_l f_2 \left(\frac{r}{r_{c,l}} \right) \quad (10)$$

$$\left(T + V_l^{(2)}(r) \right) w_l^{(2)}(r) = \tilde{\epsilon}_l w_l^{(2)}(r) \quad (11)$$

This determines the value of c_l .

Hamann-Schlüter-Chiang recipe

- ▶ The valence wf is defined as

$$\Phi_l(r) = -\gamma_l \left[w_l^{(2)}(r) + \delta_l r^{l+1} f_3 \left(\frac{r}{r_{c,l}} \right) \right] \quad (12)$$

where γ_l and δ_l are chosen such that
 $\Phi_l(r) \rightarrow \Psi_l(r)$ for $R \geq r_c$.

And

$$\gamma_l^2 \int |w_l^{(2)}(r) + \delta_l r^{l+1} f_3 \left(\frac{r}{r_{c,l}} \right)|^2 r dr = 1 \quad (13)$$

Hamann-Schlüter-Chiang recipe

- ▶ Given Φ_I and $\tilde{\epsilon}_I$ the equation:

$$(T + V^{val})|\Phi_I\rangle = \tilde{\epsilon}_I|\Phi_I\rangle.$$

is inverted to get $V^{val}(r)$.

Hamann-Schlüter-Chiang chose $f_1(x) = f_2(x) = f_3(x) = \exp[-x^4]$.

$$V_i^{PP}(r) = V_i^{val}(r) - V_H(n_V) - V_{xc}(n_V) \quad (14)$$

The total atomic pseudopotential then takes the form of a sum over all angular momentum channels:

$$V^{PP}(\mathbf{r}) = \sum_L V_L^{PP}(r) \mathbf{P}_L(\omega) \quad (15)$$

where $\mathbf{P}_L(\omega)$ is the projector on the angular momentum state L , defined by $\{l, m\}$ and ω are angular variables.

Bachelet-Hamann-Schlüter pseudopotentials

Bachelet et proposed an analytic form to fit the pseudos generated by Hamann-Schlüter-Chiang of the form:

$$V^{PP}(r) = V^{core}(r) + \sum_L \Delta V_L^{ion}(r) \quad (16)$$

$$V^{core}(r) = -\frac{Z_V}{r} \left[\sum_{i=1}^2 c_i^{core} \operatorname{erf}(\sqrt{\alpha_i^{core}} r) \right] \quad (17)$$

$$V_L^{ion}(r) = \sum_{i=1}^3 (A_i + r^2 A_{i+3}) \exp[-\alpha_i r^2] \quad (18)$$

the advantage here is that this form allow an easy implementation in plane-wave code, since the Fourier transform can be also written analytically.

Kerker pseudopotentials

In the Kerker approach² pseudopotentials are constructed to satisfy HSC conditions, but replacing the AE wf inside r_c with a smooth analytic function that matches the AE wf at r_c .

- ▶ r_c is generally larger than that used in HSC

The analytic form proposed by Kerker is

$$\Phi_l(r) = r^{l+1} \exp[p(r)] \text{ for } r < r_{c,l} \quad (19)$$

with l -dependent cut-off radii $r_{c,l}$ and

$$p(r) = \alpha r^4 + \beta r^3 + \gamma r^2 + \delta \quad (20)$$

The method of Kerker was generalized by Troullier and Martins to polynomials of higher order³

²Kerker, *J. of Phys. C* 13; L189 (1980)

³*Phys. rev. B*, 43: 1993. (1991).

An Example: pseudos for carbon

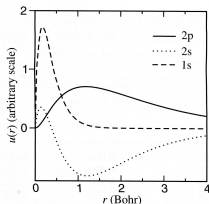


Fig. 4.6. All-electron wave functions $u(r) = r\Psi(r)$ for the carbon atom in the ground state.

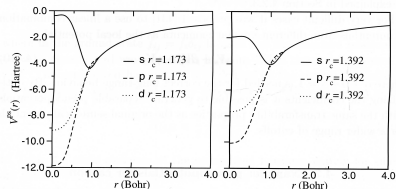
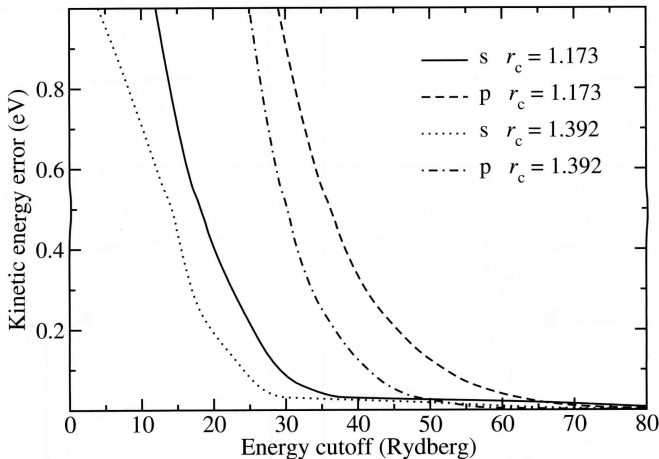


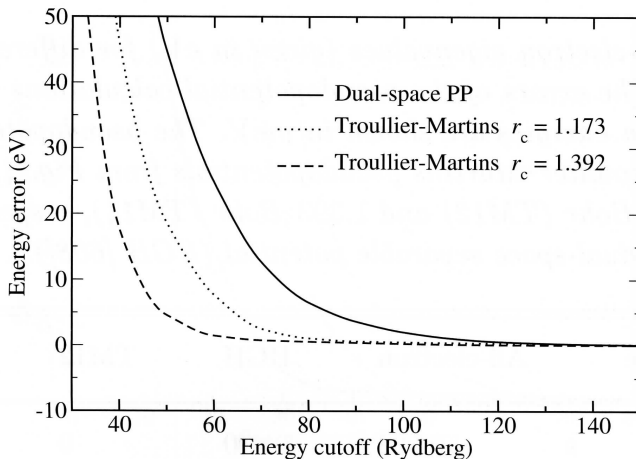
Fig. 4.7. Two sets of Troullier-Martins pseudopotentials for carbon generated by using two different cutoff radii r_c as indicated in the panels.

Martin-Troulliers
 pseudopotential for carbon in
 the LDA.

reference configuration:
 $1s^2 2s^2 2p^2$



Convergence of the kinetic energy for carbon atom as function of the cutoff.



Convergence of the total energy of diamond as function of the cutoff.

Controlling temperature: thermostats
Controlling pressure: barostats

Zero or small electronic gaps: thermostatted electrons

- ▶ One way to (try to) overcome the problem in coupling of electronic and ionic dynamics is to thermostat also the electrons (Blöchl & Parrinello, PRB 1992)
- ▶ Thus electrons cannot heat up; if they try to, thermostat will adsorb the excess heat
- ▶ Target fictitious kinetic energy $E_{kin,0}$ instead of temperature
- ▶ Mass of thermostat to be selected appropriately:
 - Too light: Adiabacity violated (electrons may heat up)
 - Too heavy: Ions dragged excessively
- ▶ Note: Introducing the thermostat the conserved quantity changes

$$M_I \ddot{\mathbf{R}}_I(t) = -\frac{\partial}{\partial \mathbf{R}_I} \langle \Psi_0 | H_e^{KS} | \Psi_0 \rangle - M_I \dot{R}_I \dot{X}_R \quad (21)$$

$$\mu \ddot{\phi}_i(t) = -H_e^{KS} \phi_i + \sum_j \Lambda_{ij} \phi_j - \mu \dot{\phi}_i \dot{X}_e \quad (22)$$

in blue are the frictional terms governed by the following equations:

$$Q_e \ddot{X}_e = 2 \left[\sum_i \mu \dot{\phi}_i^2 - E_{kin,0} \right] \quad (23)$$

$$Q_R \ddot{X}_R = 2 \left[\sum_I \frac{1}{2} M_I \dot{R}_I^2 - \frac{1}{2} g K_B T \right] \quad (24)$$

The masses Q_e and Q_R determines the time scale for the thermal fluctuations. The conserved quantity is now:

$$E_{tot} = \sum_I \frac{1}{2} M_I \dot{R}_I^2 + \sum_i \mu \langle \dot{\phi}_i | \dot{\phi}_i \rangle + \langle \Psi_0 | H_e^{KS} | \Psi_0 \rangle + \frac{1}{2} Q_e \dot{X}_e^2 + 2E_{kin,0} X_e + \frac{1}{2} Q_R \dot{X}_R^2 + g K_B T X_R \quad (25)$$

Standard Nose'-Hoover thermostat suffers from non-ergodicity problems for certain classes of Hamiltonian, so a closely related technique has been proposed, the **Nose'-Hoover chain thermostat**. For the nuclear part:

$$M_I \ddot{\mathbf{R}}_I = -\nabla E^{KS} - M_I \dot{\xi}_1 \dot{\mathbf{R}}_I \quad (26)$$

$$Q_1^n \ddot{\xi}_1 = \left[\sum_I M_I \dot{R}_I^2 - g K_B T \right] - Q_1^n \dot{\xi}_1 \dot{\xi}_2 \quad (27)$$

$$Q_k^n \ddot{\xi}_k = 2 \left[Q_{k-1}^n \dot{\xi}_{k-1}^2 - K_B T \right] - Q_k^n \dot{\xi}_k \dot{\xi}_{k+1} (1 - \delta_{kK}) \quad (28)$$

For the electronic part:

$$\mu \ddot{\phi}_i = -H_e^{KS} \phi_i + \sum_{ij} \Lambda_{ij} \phi_j - \mu \dot{\eta}_1 \dot{\phi}_i \quad (29)$$

$$Q_1^e \ddot{\eta}_1 = \left[\sum_i^{occ} \mu \langle \phi_i | \phi_i \rangle - T_1^0 \right] - Q_1^e \dot{\eta}_1 \dot{\eta}_2 \quad (30)$$

$$Q_l^n \ddot{\eta}_l = 2 \left[Q_{l-1}^n \dot{\eta}_{l-1}^2 - \frac{1}{\beta_e} \right] - Q_l^e \dot{\eta}_l \dot{\eta}_{l+1} (1 - \delta_{lL}) \quad (31)$$

- ▶ Separate chains composed of K and L coupled thermostats are attached to the nuclear and electronic equations of motion, respectively
- ▶ Masses for the thermostats are chosen so that there overlap of the thermostat and system power spectra.

$$Q_1^n = \frac{gK_B T}{\omega_n^2}, \dots Q_k^n = \frac{gK_B T}{\omega_n^2}, \quad (32)$$

$$Q_1^e = \frac{2T_e^0}{\omega_e^2}, \dots Q_l^e = \frac{2T_e^0}{\omega_e^2} \quad (33)$$

- ▶ massive thermostatting method: NH chains for individual nuclear degree of freedom. Accelerate expensive equilibration periods

Energy and Momentum conservation

In micro-canonical classical molecular simulations the total energy and the total momentum are conserved.

In the case of thermostatted NVT simulations the constant of motion is:

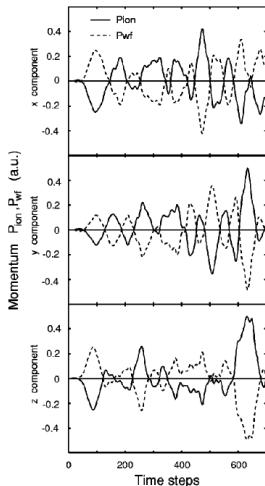
$$E_{cons}^{NVT} = \sum_i^{occ} \mu \langle \dot{\phi}_i | \dot{\phi}_i \rangle + \sum_I \frac{1}{2} M_I \dot{\mathbf{R}}_I^2 + E^{KS} [\{\phi_i\}, \{\mathbf{R}_I\}] \quad (34)$$

$$+ \sum_{l=1}^L \frac{1}{2} Q_l^e \dot{\eta}_l^2 + \sum_{l=2}^L \frac{\eta_l}{\beta_e} + 2T_e^0 \eta_1 + \sum_{k=1}^K \frac{1}{2} Q_k^n \dot{\xi}_k^2 + \sum_{k=2}^K K_b T \xi_k + g K_b T \xi_1 \quad (35)$$

In micro-canonical CPMD a generalized linear momentum is conserved:

$$\mathbf{P}_{CP} = \mathbf{P}_n + \mathbf{P}_e = \sum_I \mathbf{P}_I + \sum_i^{occ} \mu \langle \dot{\phi}_i | -\frac{1}{2} \nabla_r | \phi_i \rangle + c.c. \quad (36)$$

where $\mathbf{P}_I = M_I \dot{\mathbf{R}}_I$.



Time evolution of P_{ion} (solid line) and P_{wf} (dashed line) in the diamond structure of Si. From the upper panel, three components, x, y, z, are shown, respectively. (Morishita and Nosé' *Phys Rev B*, 59, 15126 (1999))

Imposing pressure: barostats

Original version from Andersen⁴ devised to allow isotropic fluctuations in the volume of the supercell. **Variable cell approach**: allows structural phase transition in solids at finite temperature. Parrinello-Rahman⁵ Built an extended Lagrangian with additional dynamical variables $\mathbf{a}_1, \mathbf{a}_2, \mathbf{a}_3$, the primitive Bravais lattice vectors. Using the 3×3 matrix $\mathbf{h} = [\mathbf{a}_1, \mathbf{a}_2, \mathbf{a}_3]$ which define the volume Ω , the scaled coordinates \mathbf{S} are defined by $\mathbf{R}_I = \mathbf{h}\mathbf{S}_I$. the normalized original orbitals are transformed according to:

$$\phi_i(\mathbf{r}) = \frac{1}{\Omega} \phi_i(\mathbf{s}) \quad (37)$$

The cell-variable extended Lagrangian is:

$$\begin{aligned} \mathcal{L} = & \sum_i \mu \langle \dot{\phi}(\mathbf{s})_i | \dot{\phi}_i(\mathbf{s}) \rangle - E^{KS}[\{\phi_i\}, \{\mathbf{h}\mathbf{S}_I\}] \\ & + \sum_{ij} \Lambda_{ij} (\langle \phi_i(\mathbf{s}) | \phi_j(\mathbf{s}) \rangle - \delta_{ij}) + \sum_I \frac{1}{2} M_I (\mathbf{S}_I^T \mathbf{h}^T \mathbf{h} \mathbf{S}_I) + \frac{1}{2} W \text{Tr} \mathbf{r} \mathbf{h}^T \dot{\mathbf{h}} - p\Omega \end{aligned} \quad (38)$$

$$\begin{aligned} \mathcal{L} = & \sum_i \mu \langle \dot{\phi}(\mathbf{s})_i | \dot{\phi}_i(\mathbf{s}) \rangle - E^{KS}[\{\phi_i\}, \{\mathbf{h}\mathbf{S}_I\}] \\ & + \sum_{ij} \Lambda_{ij} (\langle \phi_i(\mathbf{s}) | \phi_j(\mathbf{s}) \rangle - \delta_{ij}) + \sum_I \frac{1}{2} M_I (\dot{\mathbf{S}}_I^T \mathbf{h}^T \mathbf{h} \dot{\mathbf{S}}_I) + \frac{1}{2} W \text{Tr} \dot{\mathbf{h}}^T \dot{\mathbf{h}} - p\Omega \end{aligned} \quad (39)$$

- ▶ nine additional degrees of freedom associated with lattice vectors of supercell \mathbf{h} .
- ▶ This constant-pressure CPMD reduce to constant-volume CPMD in the limit $\dot{\mathbf{h}} \rightarrow 0$ (apart from a constant term $p\Omega$)
- ▶ W is the fictitious mass that controls the timescale of the cell dynamics

The resulting equations of motion are:

$$M_I \ddot{S}_{I,u} = - \sum_{v=1}^3 \frac{\partial E^{KS}}{\partial R_{I,v}} (\mathbf{h}^T)_{v,u}^{-1} - M_I \sum_{v=1}^3 \sum_{s=1}^3 \mathcal{G}_{uv}^{-1} \dot{\mathcal{G}}_{vs} \dot{S}_{I,s} \quad (40)$$

$$\mu \ddot{\phi}_i(\mathbf{s}) = - \frac{\partial E^{KS}}{\partial \phi_i^*(\mathbf{s})} + \sum_j \Lambda_{ij} \phi_j(\mathbf{s}) \quad (41)$$

$$W \ddot{h}_{uv} = \Omega \sum_{s=1}^3 (\Pi_{us}^{tot} - p \delta_{us}) (\mathbf{h}^T)_{sv}^{-1} \quad (42)$$

where the total stress tensor is:

$$\Pi_{us}^{tot} = \frac{1}{\Omega} \sum_I M_I (\dot{\mathbf{S}}_I^T \mathcal{G} \dot{\mathbf{S}}_I)_{us} + \Pi_{us} \quad (43)$$

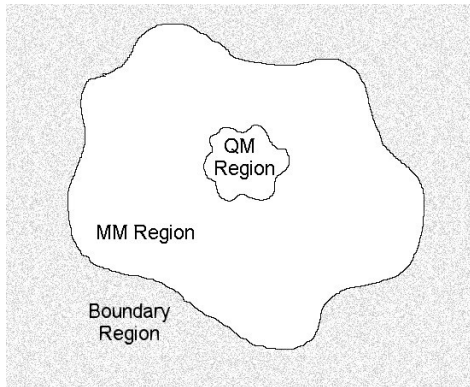
and Π_{us} is electronic stress tensor:

$$\Pi_{us} = - \frac{1}{\Omega} \sum_v \frac{\partial E_{tot}}{\partial h_{uv}} h_{vs}^T \quad (44)$$

- ▶ frictional feedback mechanism
- ▶ Parrinello-Rahman used in connection with metadynamics
- ▶ practical issue: basis set error, when using a fixed cutoff in plane wave with a varying cell

Alternative approach for clusters⁶.

Idea: surrounding the finite cluster by a pressurizing medium described by N_L classical point particles.ⁱ (e.g. liquid of purely repulsive soft spheres).



⁶R. Martonak, C. Molteni and M. Parrinello, *Comp Mat Science* 20 (3-4) 2001, 293-299

Alternative approach for clusters⁷.

Idea: surrounding the finite cluster by a pressurizing medium described by N_L classical point particles. i (e.g. liquid of purely repulsive soft spheres).
 The corresponding Lagrangian is:

$$\mathcal{L} = \sum_I \frac{1}{2} M_I \dot{\mathbf{R}}_I^2 + \sum_i \mu \langle \dot{\phi}(\mathbf{r})_i | \dot{\phi}_i(\mathbf{r}) \rangle - E^{KS}[\{\phi_i\}, \{\mathbf{R}_I\}] \quad (45)$$

$$+ \sum_{ij} (\langle \phi(\mathbf{r})_i | \phi_j(\mathbf{r}) \rangle - \delta_{ij}) + \sum_{\alpha} \frac{1}{2} M_{\alpha} \dot{\mathbf{X}}_{\alpha}^2 \quad (46)$$

$$+ - \sum_{I, \alpha} V_{C-L}(|\mathbf{R}_I - \mathbf{X}_{\alpha}|) - \sum_{\alpha < \beta} V_{L-L}(|\mathbf{X}_{\alpha} - \mathbf{X}_{\beta}|) \quad (47)$$

where M_{α} is the mass of a liquid particle at position \mathbf{X}_{α} and V_{C-L} and V_{L-L} are model pair potential to describe the cluster-liquid and the liquid-liquid interactions.

⁷R. Martonak, C. Molteni and M. Parrinello, Comp Mat Science 20 (3-4) 2001, 293-299

How is the pressure controlled?

For purely repulsive soft spheres:

$$V_{L-L}(r) = \epsilon_{L-L} \left(\frac{\sigma_{L-L}}{r} \right)^{12} \quad (48)$$

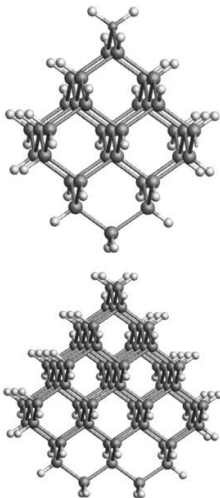
the equation of state gives:

$$p = \frac{N_L K_B T}{\Omega_L} \xi(\tilde{\rho}) \quad (49)$$

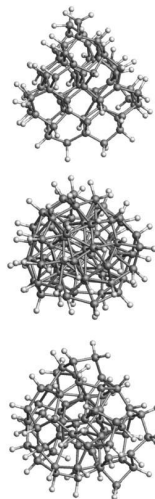
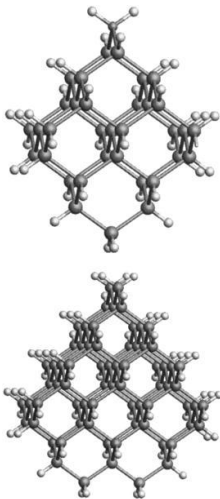
where

$$\xi(\tilde{\rho}) = \frac{N_L}{\Omega_L} \frac{\sigma_{L-L}^3}{\sqrt{2}} \left(\frac{\epsilon_{L-L}}{K_B T} \right)^{1/4} \quad (50)$$

the pressure is adjusted tuning ϵ_{L-L} .

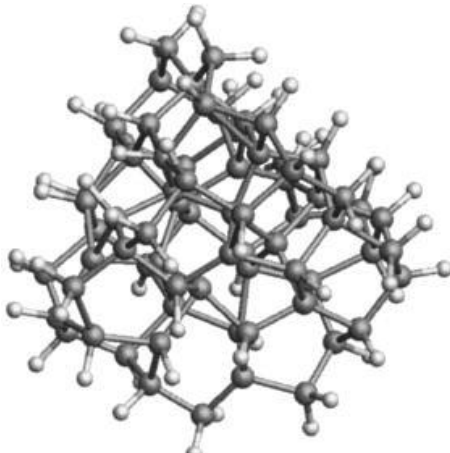


$Si_{35}H_{36}$ at 25 GPa (top), 35 GPa (center), and 5 GPa (after the

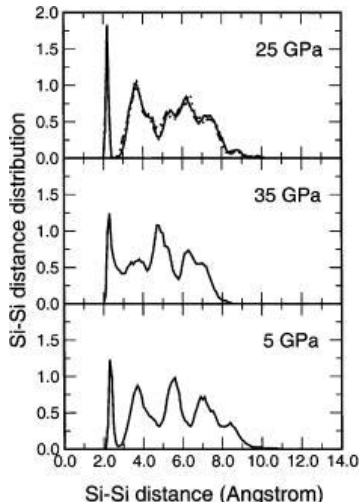


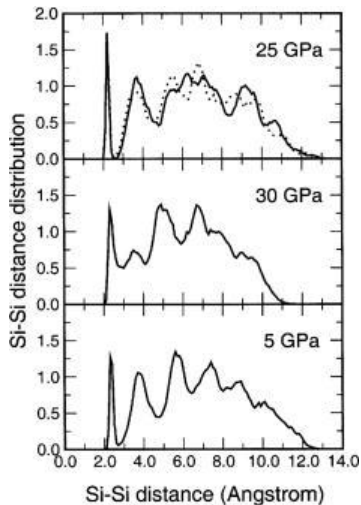
$Si_{71}H_{60}$ at 25 GPa (top), 30 GPa (center), and 5 GPa (after the

In both clusters, up to 25 GPa, a distorted but predominantly tetrahedral coordination is maintained, with no sign of a transformation to a different structure. This also holds for the case with the vacancy, even if with a higher degree of disorder.

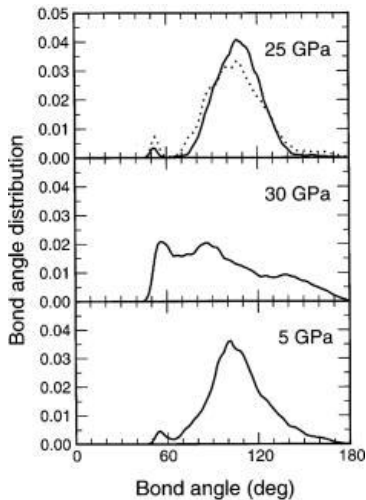
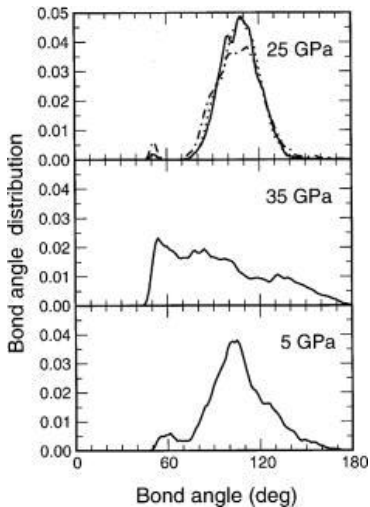


Dramatic structural transformation occurs for $\text{Si}_{35}\text{H}_{36}$ at 35 GPa and for $\text{Si}_{71}\text{H}_{60}$ at 30 GPa. Shape changes to roughly spherical and the tetrahedral coordination is no longer dominant. (In accord with expts.)



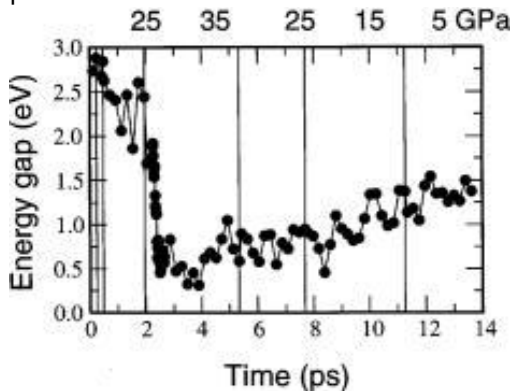


Distributions of the SiSi distances for Si₇₁H₆₀



The change in coordination and shape is accompanied by a change in the electronic properties.

There is a clear qualitative trend toward metallicity at high pressure.



Time evolution of the Kohn-Sham energy gap of Si₃₅H₃₆